ARTICLE
Journal of Cellular Biochemistry 109:434–446 (2010)

Journal of Cellular Biochemistry

# Glycolytic Pyruvate Regulates P-Glycoprotein Expression in Multicellular Tumor Spheroids via Modulation of the Intracellular Redox State

Maria Wartenberg,[1] Madeleine Richter,[1] André Datchev,[1] Sebastian Günther,[2] Nada Milosevic,[3] Mohamed M. Bekhite,[1] Hans-Reiner Figulla,[1] Josep M. Aran,[4] Jordi Pétriz,[5] and Heinrich Sauer[3*]

[1]*Department of Internal Medicine I, Cardiology Division, Friedrich Schiller University, Jena, Germany*

[2]*Institute of Microbiology and Epizootics, Veterinary Faculty, Free University, Berlin, Germany*

[3]*Department of Physiology, Justus Liebig University, Giessen, Germany*

[4]*Medical and Molecular Genetics Center, Institut d'Investigació Biomèdica de Bellvitge (IDIBELL), Hospital Duran i Reynals, L'Hospitalet de Llobregat, Barcelona, Spain*

[5]*Institut de Recerca, Hospital Universitari, Vall d'Hebron, Barcelona, Spain*

## ABSTRACT

ABC transporters like P-glycoprotein (P-gp/ABCB1) are membrane proteins responsible for the transport of toxic compounds out of non-malignant cells and tumor tissue. Aim: To investigate the effect of glycolysis and the tissue redox state on P-gp expression in multicellular tumor spheroids derived from prostate adenocarcinoma cells (DU-145), glioma cells (Gli36), and the human cervix carcinoma cell line KB-3-1 transfected with a P-gp–EGFP fusion gene that allows monitoring of P-gp expression in living cells. During cell culture of DU-145, Gli36, and KB-3-1 tumor spheroids P-gp expression was observed as well as increased lactate and decreased pyruvate levels and expression of glycolytic enzymes. Inhibition of glycolysis for 24 h by either iodoacetate (IA) or 2-deoxy-D-glucose (2-DDG) downregulated P-gp expression which was reversed upon coincubation with the radical scavenger ebselen as shown by semi-quantitative immunohistochemisty in DU-145 and Gli36 tumor spheroids, and by EGFP fluorescence in KB-3-1 tumor spheroids. Consequently endogenous ROS generation in DU-145 tumor spheroids was increased in the presence of either IA or 2-DDG, which was abolished upon coincubation with ebselen. Exogenous addition of pyruvate significantly reduced ROS generation, increased P-gp expression as well as efflux of the P-gp substrate doxorubicin. Doxorubicin transport was significantly blunted by 2-DDG and IA, indicating that inhibition of glycolysis reversed the multidrug resistance phenotype. In summary our data demonstrate that P-gp expression in tumor spheroids is closely related to the glycolytic metabolism of tumor cells and can be downregulated by glycolysis inhibitors via mechanisms that involve changes in the cellular redox state. J. Cell. Biochem. 109: 434–446, 2010. 

**KEY WORDS:** GLYCOLYSIS; MULTIDRUG RESISTANCE; P-GLYCOPROTEIN; REACTIVE OXYGEN SPECIES

Intrinsic chemotherapeutic resistance developing prior to chemotherapy as well as acquired resistance occurring after several cycles of chemotherapy appears in several types of solid human tumors and is related to the expression of ABC transporters, the most clinically relevant being P-glycoprotein (P-gp) which is also named ABCB1 [Sharom, 2008]. Previously it has been demonstrated that P-gp expression is regulated by the hypoxic state within solid tumors which is characterized by upregulation of hypoxia-induced factor 1α (HIF-1α) [Comerford et al., 2002; Wartenberg et al., 2003], a key regulator of several enzymes involved in the glycolytic pathway. Cancer cells generally exhibit increased glycolysis for ATP generation (the Warburg effect) due in part to mitochondrial respiration injury and hypoxia [DeBerardinis, 2008]. Both of them are frequently associated with resistance to therapeutic agents, indicating that expression of P-gp and the metabolic switch of tumor cells from oxidative phosphorylation

Grant sponsor: Federal Institute for Risk Assessment (BfR); Grant number: BFR-ZEBET-1328-181; Grant sponsor: Excellence Cluster Cardiopulmonary System.

*Correspondence to: Prof. Dr. Heinrich Sauer, Department of Physiology, Justus Liebig University Giessen, Aulweg 129, 35392 Giessen, Germany. E-mail: heinrich.sauer@physiologie.med.uni-giessen.de

Received 26 September 2009; Accepted 16 October 2009 • DOI 10.1002/jcb.22422 • © 2009 Wiley-Liss, Inc.
Published online 30 November 2009 in Wiley InterScience (www.interscience.wiley.com).

towards glycolysis may be closely related. This makes sense since expression of multidrug resistance (MDR) transporters and the glycolytic metabolism enable tumor cells to proliferate even in a hypoxic tissue microenvironment and high concentrations of potentially toxic catabolic waste products which are efficiently extruded from the tumor tissue.

Previous studies of us have indicated that P-gp expression can be downregulated and the MDR phenotype reversed by low concentrations of ROS acting as signaling molecules [Wartenberg et al., 2000, 2001b, 2003, 2005]. Others have shown that high concentrations of ROS causing oxidative stress on the contrary upregulate P-gp by signaling pathways involving among others ROS-mediated activation of JNK and nuclear factor-κB [Thevenod et al., 2000; Bentires-Alj et al., 2003]. ROS are continuously generated in growing cancer cells and may be involved in signaling pathways regulating cell proliferation and the development of drug resistance [Sauer et al., 2001]. They are mainly produced within the mitochondrial respiratory chain and by the activity of NADPH oxidases which have been previously shown to be expressed in tumors [Wu, 2006] and regulate the cell invasion capability [Chaiswing et al., 2008]. The metabolic switch towards glycolysis which is associated with inhibition of oxidative phosphorylation, presumably at least partially by induction of pyruvate dehydrogenase kinase 1 (PDK1) through HIF-1 [Dang, 2007], should be paralleled by a downregulation of ROS generation. Furthermore the relationship between therapeutic resistance and glycolysis may at least partially be due to the radical scavenging potential of glycolytic intermediates, mainly pyruvate and to the link between this metabolite and the cellular redox status [Sattler et al., 2007]. In accordance with this we have previously shown that in tumor spheroids ROS are downregulated with increasing size of the tumors and the acquirement of a MDR phenotype. Under these conditions HIF-1α and P-gp were upregulated and drugs were efficiently extruded [Wartenberg et al., 2003].

Although the Warburg effect is known for many decades, therapeutic approaches to treat cancer by inhibition of glycolytic pathways are only recently emerging [DeBerardinis, 2008]. Drugs able to perturb cancer cell metabolism, specifically at the level of glycolysis may display interesting therapeutic activities in cancer. Drug actions on cell metabolism could be related to the inhibition of energetic and anabolic processes, the reduction of hypoxia-associated MDR and the reduction of ATP-dependent drug resistance [Scatena et al., 2008]. Reversal of the MDR phenotype by downregulation of MDR transporters and inhibition of ATP-dependent drug transporters like P-gp could chemosensitize tumors towards conventional anti-cancer agents. Currently several glycolytic inhibitors are in preclinical and clinical development and may be utilized in future cancer treatment [Denko, 2008]. To properly estimate the efficacy of glycolytic inhibitors to decelerate the growth of cancer cells and understand their mechanisms of action a deepened knowledge of MDR pathways associated with the Warburg effect is necessary. Against this background the present study was designed. We demonstrate that growing tumors acquire the MDR phenotype and express P-gp concomitant with metabolic changes towards anaerobic glycolysis. Inhibition of glycolysis raises intracellular ROS, downregulates P-gp expression and reverses the MDR phenotype. Hence the data of the present study demonstrate a link between drug resistance and the glycolytic metabolism of tumor cells and suggest how MDR can be reversed and tumor cell growth inhibited by interference with the glycolytic cell metabolism.

## MATERIALS AND METHODS

### CULTURE TECHNIQUE OF MULTICELLULAR SPHEROIDS

The human prostate cancer cell line DU-145 was grown routinely in 5% $CO_2$/humidified air at 37°C with Ham's F10 medium (Gibco, Helgerman Court, MD) supplemented with 10% fetal bovine serum (FBS) (Gibco), 2 mM L-glutamine, 0.1 mM 2-mercaptoethanol, 2 mM non-essential amino acids (NEA), 100 U/ml penicillin and 50 μg/ml streptomycin. The drug sensitive KB-3-1 cell line derived from human HeLa cervix carcinoma cells and the glioma Gli36 cell line were cultured in Dulbecco's modified Eagle's medium (DMEM) with 10% FBS, 2 mM L-glutamine, 100 U/ml penicillin, 100 μg/ml streptomycin, 10 μM sodium pyruvate. Spheroids were grown from single cells. Cell monolayers were enzymatically dissociated with 0.1% trypsin and 0.05% EDTA (Gibco), seeded in siliconated 250 ml spinner flasks (Tecnomara, Fernwald, Germany) with 250 ml complete medium and agitated at 20 strokes/min using a Cellspin stirrer system (Integra Biosciences, Fernwald, Germany). Cell culture medium was partially (100 ml) changed every day. For incubation with glycolysis inhibitory agents, large multicellular tumor spheroids (diameter 250 ± 50 μm) were transferred to bacteriological tissue culture plates (diameter 10 cm) filled with 10 ml F10 cell culture medium. They were subsequently treated for 24 h with 2-deoxy-D-glucose (2-DDG) or iodoacetate (IA) (both from Sigma, Deisenhofen, Germany).

### IMMUNOHISTOCHEMISTRY

Fluorescence recordings were performed by means of a confocal laser scanning setup (LSM 410; Carl Zeiss, Jena, Germany) equipped with a 488 nm/514 nm argon-ion laser and a 543 nm He/Ne laser. The confocal setup was connected to an inverted microscope (Axiovert 135, Carl Zeiss). Antibody staining was performed on whole-mount multicellular spheroids. Spheroids were fixed with a methanol/acetone solution (at −20°C) or with paraformaldehyde (at 4°C). After washing with phosphate-buffered saline (PBS) supplemented with either 0.1% or 0.01% Triton X-100 (PBST) the spheroids were permeabilized with 1% PBST. To prevent unspecific binding the spheroids were blocked with a solution of PBS containing 10% fat-free milk powder for 1 h. Subsequently they were stained with anti-P-gp antibody (clone Ab-1) (10 μg/ml) (Calbiochem, Bad Soden, Germany) in 0.01% PBST and were incubated at room temperature for 2 h. After washing three times in PBST, spheroids were incubated for 60 min in PBS supplemented with 10% milk powder and a Cy5-conjugated goat anti-rabbit IgG (Dianova, Hamburg, Germany), concentration 15 μg/ml. Excitation was performed using a 633 nm helium–neon laser of the confocal setup. Emission was recorded using a LP655 nm filter set.

### ISOLATION OF RNA

All isolation steps were performed at room temperature. A volume of approximately 100 μl spheroids was transferred to 2 ml tubes and spun down at 80*g* for 2 min. After removal of the supernatant 1 ml Trizol (Sigma) was added and the pellet was homogenized. After incubating for 5 min 200 μl chloroform was added and shaken intensively for 20 s. After incubating for another 3 min the sample was spun down (12,000*g*, 4°C, 15 min). The RNA-containing upper phase was treated with 200 μl chloroform and spun down again (12,000*g*, 4°C, 5 min). The upper phase was transferred into a 2 ml tube and RNA was precipitated with 500 μl isopropanol. After washing with ethanol (75%) the pellet was air-dried and re-suspended in 30 μl RNase free water.

### REVERSE TRANSCRIPTASE–POLYMERASE CHAIN REACTION (RT-PCR) AND QUANTITATIVE REAL-TIME PCR

Gene expression profiles of *pyruvate dehydrogenase A1* (PDHA1), *hexokinase 1* (HK1), and *lactate dehydrogenase A* (LDHA) were monitored by RT-PCR and quantified by means of real-time PCR. Isolated total RNA was reverse-transcribed using random oligo dT-primers [Prom II Transcription System (Promega, Mannheim, Germany)]. cDNA aliquots corresponding to 50 ng total RNA were semi-quantitatively analyzed using sense and anti-sense primers of the respective genes and analyzed with real-time PCR (Applied Biosystems 7500, Applied Biosystems, Carlsbad, CA). The used sequence for sense and anti-sense primers are listed below. Real-time PCR was performed in the presence of sense and anti-sense primers for the ''housekeeping'' gene β-tubulin. Relative gene expression of the examined genes was normalized to the expression of the housekeeping gene.

HK1: forw. GGACTGGACCGTCTGAATGT; rev. ACAGTTCCTTCACC-GTCTGG
LDHA: forw. ACCCAGTTTCCACCATGATT; rev. CCCAAAATGCAA-GGAACACT
PDHA1: forw. GAACAGCAATCTTGCCAGTG; rev. CTCTTCCAAA-GGTGGCTCAG
β-tubulin: forw. AATGGCCACTCTCCTTATCAG; rev. GGCCTCGT-TGTCAATGCAATA

### DETERMINATION OF INTRACELLULAR ROS LEVELS

Intracellular ROS levels were measured using the fluorescence dye 2′7′-dichlorodihydrofluorescein diacetate ($H_2$DCFDA) (Invitrogen, Karlsruhe, Germany), which is a non-polar compound that is converted into a non-fluorescent polar derivative ($H_2$DCF) by cellular esterases after incorporation into cells. $H_2$DCF is membrane impermeable and rapidly oxidized to the highly fluorescent 2′7′-dichlorofluorescein (DCF) in the presence of intracellular ROS. For the experiments, multicellular tumor spheroids were incubated for 24 h with either IA (10 μM) or 2-DDG (5 μM). Subsequently they were immersed in E1 medium containing (in mM) NaCl 135, KCl 5.4, $CaCl_2$ 1.8, $MgCl_2$ 1, glucose 10, HEPES 10 (pH 7.4 at 23°C), and 20 μM $H_2$DCFDA dissolved in dimethyl sulfoxide (DMSO) was added. Intracellular DCF fluorescence (corrected for background fluorescence) was recorded every 5 min for a 20 min time period.

### DIFFUSION STUDIES WITH DOXORUBICIN

The anthracycline doxorubicin is a substrate of P-gp. In multidrug resistant cells the efflux of doxorubicin out of the cell should be enhanced in comparison to non-resistant cells. After treatment of the spheroids for 1 h with the glycolysis inhibiting agents 2-DDG (5 μM) and IA (10 μM) either in the presence or absence of the free radical scavenger ebselen, the samples were washed with E1 solution. Subsequently 5 μM doxorubicin–E1 solution was added and incubated for 90 min at 37°C. Thereafter doxorubicin was removed via a washing step and the fluorescence was determined after 30 min using the 543 nm He/Ne laser of the confocal setup. The difference in fluorescence grey level values (recorded with a 570 nm long pass filter set) after the 90 min incubation period (time 0) and 30 min after removal of doxorubicin from the incubation medium is indicative for the retention of doxorubicin in the cells.

### DEAD CELL STAINING

To assess the cytotoxicity of a substance, dead cell staining was carried out by the use of the dead cell stain Sytox green (Molecular Probes, Eugene, OR). After the treatment of the spheroids with glycolysis inhibiting agents the samples were incubated for 30 min in 10 ml medium containing 0.5 μM Sytox green, which is cell membrane impermeable and intensively stains the cell nuclei of dead cells with compromised cell membranes after intercalation into DNA. Sytox green fluorescence was excited by an argon-ion laser (488 nm) of the confocal setup. Emission was recorded using a 515-nm long pass filter set.

### DETERMINATION OF LACTATE AND PYRUVATE

Measurement of lactate concentration was performed applying the Sigma assay kit (Sigma) based on lactate peroxidase which catalyses the reaction of lactate to pyruvate and $H_2O_2$. In the presence of $H_2O_2$ peroxidase is catalyzing the oxidative condensation of chromogenic precursors which are analyzed at 540 nm. In the pyruvate assay pyruvate is oxidized by lactate dehydrogenase (LDH) via the reaction: pyruvate + NADH≡lactate + $NAD^+$. The reduction of absorbance at 340 nm due to oxidation of NADH becomes a measure of the pyruvate concentration. In brief, spheroids were transferred in 1.5 ml tubes and spun down at 80*g* (1 min). The supernatant was discarded. After determination of the dry mass, a fivefold volume of *aqua dest* was added to the tubes. The spheroids were homogenized with a pipette and the homogenate spun down at 10,000*g* (1 min). Several fast cooling/melting-steps completed the cell disruption. After adding the 2-fold amount of perchloric acid (PCA) (8%) the samples were mixed for 30 s and cooled on ice for 5 min. A centrifugation step at 1,500*g* for 10 min followed. Subsequently analysis was performed according to the instructions of the manufacturer.

### DETERMINATION OF P-gp–EGFP EXPRESSION BY THE OPTICAL PROBE TECHNIQUE

Radial recordings of P-gp–EGFP fluorescence were obtained from 10-day-old KB-3-1 multicellular tumor spheroids in selected regions of interest within the center of the tumor spheroids as previously described [Wartenberg et al., 1998b]. Recording was started in the center of the spheroid and moving to the periphery.

The motor commands of the stepper motor of the confocal setup were chosen to give 10 μm steps. The pinhole settings were set to provide a full width maximum of 8 μm. Each ROI was scanned once in 0.064 s. The mean field intensity of the fluorescence signal was determined in each ROI and the fluorescence intensity data were plotted as a function of the penetration depth of the laser beam in the tissue. In order to correct the measured fluorescence intensity traces for fluorochrome and depth-dependent light absorption and scattering, attenuation coefficients C were determined using EGFP-labeled densely packed cell pellets obtained from enzymatically dissociated KB-3-1 tumor spheroids. To address depth-dependent heterogeneities of fluorochrome distributions in tumor spheroids, the fluorescence intensity traces obtained from intact tumor spheroids were set into relation with fluorescence intensities traces from densely packed cell pellets; this resulted in a fluorescence distribution coefficient $D = I/I_{cal}$. The correction for light attenuation within KB-3-1 tumor spheroids was performed using the following algorithm: $\ln [I_{corr.}] = \ln [I] + CDz$, where $I_{corr.}$ is the fluorescence intensity after correction for light attenuation in a

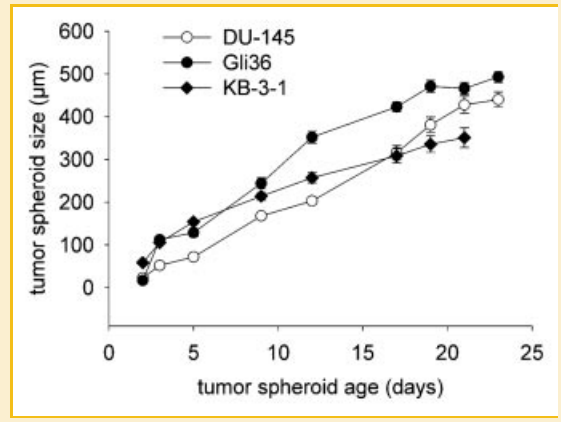


Fig. 1. Growth kinetics of multicellular tumor spheroids of the DU-145 prostate cancer cell line, the Gli36 glioma cell line and the KB-3-1 human cervix carcinoma cell line. Tumor spheroids were cultivated in spinner flask technique and spheroid diameters evaluated by microscopic inspection.

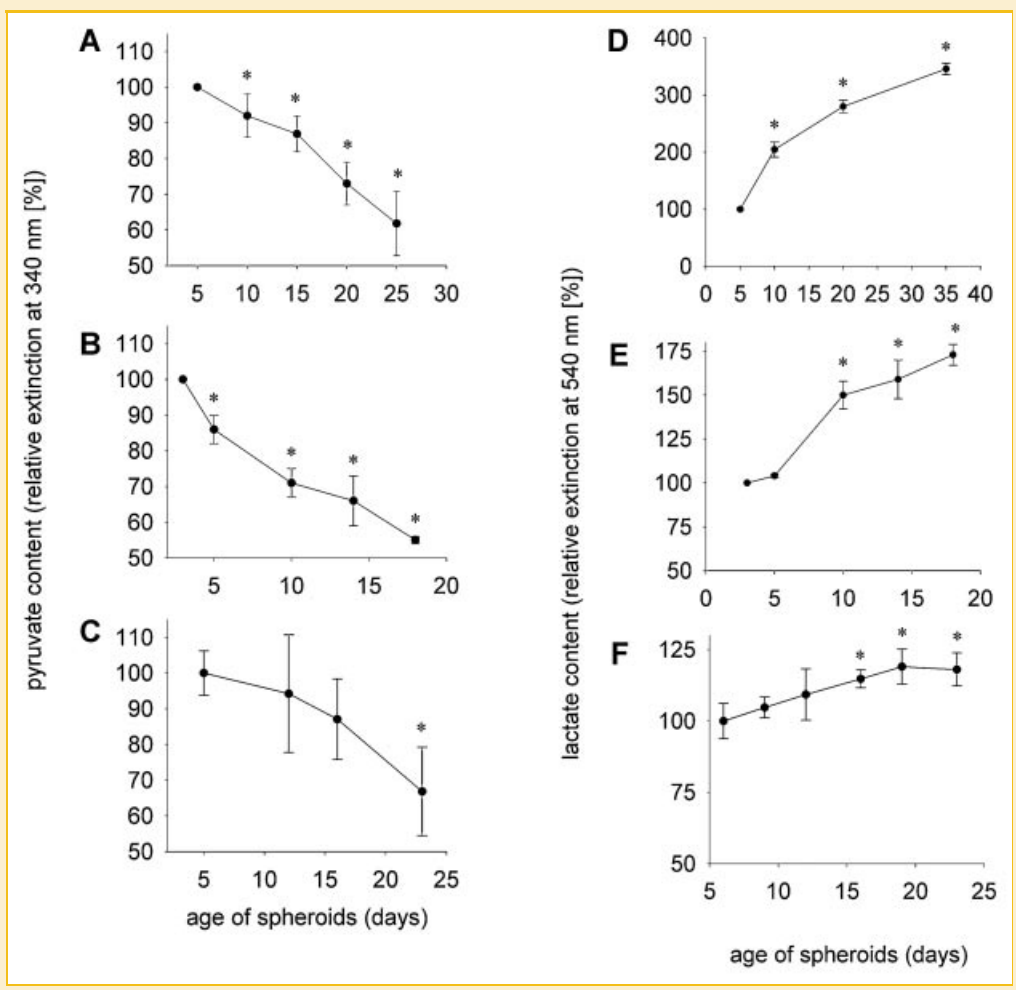


Fig. 2. Pyruvate (A–C) and lactate (D–F) content in DU-145 (A,D), Gli36 (B,E), and KB-3-1 (C,F) tumor spheroids with increasing age in cell culture. It is evident that pyruvate generation is decreasing at cost of lactate production. This reflects the increased hypoxia occurring in the avascular growing tissues. $^{*}P < 0.05$, statistically different as compared to the first point in the curve (one-way ANOVA).

discrete depth z within the EGFP-labeled tissue and I is the fluorescence intensity before correction. The fluorescence distribution $D = I/I_{cal}$ was obtained by dividing the measured fluorescence intensity I at a discrete depth z of the laser beam in the tumor spheroid by the respective intensity value $I_{cal}$ in the calibration function.

### STATISTICAL ANALYSIS

Either one-way ANOVA or Student's *t*-test for unpaired data were applied as appropriate. A value of $P < 0.05$ was considered significant.

## RESULTS

### CHANGES IN PYRUVATE AND LACTATE CONTENT IN MULTICELLULAR TUMOR SPHEROIDS

During the growth of avascular micrometastases the center of the tissue becomes hypoxic which results in a proliferation gradient with vital cells at the tumor periphery and quiescent and necrotic cell layers towards the center [Mueller-Klieser, 1997]. Under hypoxic conditions pyruvate generated from glucose during glycolysis is metabolized by LDH to lactate. Hence increasing hypoxia in growing tumor spheroids should be accompanied by a decrease in pyruvate content and increase in lactate content. In the present study the growth of multicellular tumor spheroids of the DU-145 prostate cancer cell line, the Gli36 glioma cell line and the human cervix carcinoma cell line KB-3-1 transfected with a P-gp–EGFP fusion gene to monitor P-gp fluorescence in living cells was assessed (see Fig. 1, n = 3) and correlated to intracellular pyruvate and lactate contents (see Fig. 2A–F). Indeed determination of pyruvate and lactate content in multicellular tumor spheroids of the DU-145 prostate cancer cell line (Fig. 2A,D; n = 3), the Gli36 glioma cell line (Fig. 3B,E; n = 3) and the KB-3-1 cell line (Fig. 2C,F; n = 3) revealed that during the growth of the spheroids the pyruvate content constantly decreased whereas an increase in lactate content was observed, thus suggesting an increase of anaerobic glycolysis with increasing size of tumor spheroids.

The metabolic switch towards glycolysis occurring in hypoxic regions of the tumor tissue should be accompanied by changes in mRNA expression of enzymes involved in glycolytic pathways. In the present study mRNA expression of *LDHA*, *PDHA1* and *HK1* which catalyze the metabolism of pyruvate to lactate, pyruvate to acetyl-CoA and the phosphorylation of glucose to glucose-6-phosphate, respectively, was assessed (Fig. 3A–F). For this investigation the DU-145 (see Fig. 3A–C; n = 3) and the KB-3-1 (see Fig. 3D–F; n = 3) cell lines were selected. The data of the present study demonstrate that all glycolytic enzymes investigated in the present study were upregulated between day 12 and days 22–25 of

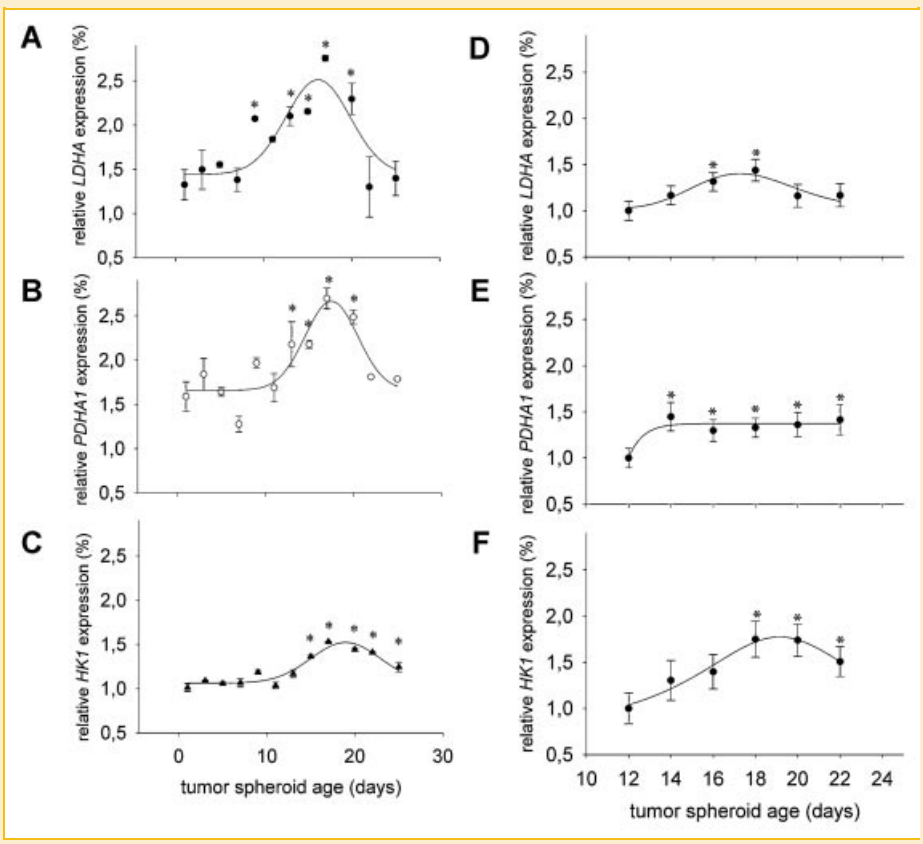


Fig. 3. mRNA expression of the glycolytic enzymes LDHA (A,D), PDHA1 (B,E), and HK1 (C,F) with increasing age of DU-145 (A–C) and KB-3-1 (D–F) multicellular tumor spheroids. The expression of glycolytic enzymes is increasing until approximately days 18–20. This is the time where central necrosis develops which results in a decline in metabolic activity. $^{*}P < 0.05$, statistically different as compared to days 1 of cell culture (one-way ANOVA).

cell culture, thus suggesting that in hypoxic multicellular tumor spheroids glycolytic pathways are upregulated as previously demonstrated in vivo [Sattler et al., 2007].

## EXPRESSION OF P-gp DURING THE GROWTH OF TUMOR SPHEROIDS

We have previously reported on the development of an intrinsic P-gp-dependent drug resistance in multicellular tumor spheroids of different origin and have outlined a role of hypoxia and ROS in this process [Wartenberg et al., 1998a, 2000, 2001b]. However, a relation between glycolysis, ROS, and P-gp in tumor spheroids was not investigated. In the present study we assessed P-gp expression by semi-quantitative immunohistochemistry in DU-145 and Gli36 tumor spheroids and additionally in the human cervix carcinoma cell line KB-3-1 transfected with a P-gp–EGFP fusion gene that allows monitoring of P-gp expression in living cells [Petriz et al., 2004]. As previously shown [Wartenberg et al., 2001b] a transient upregulation of P-gp was observed between days 4 and 13 in DU-145 and between days 4 and 6 in Gli36 tumor spheroids which paralleled the development of quiescent, cell proliferation-inactive cell areas in these tumors (Fig. 4A,B; n = 3). In KB-3-1 tumor spheroids an increase in EGFP fluorescence was observed with increasing growth of tumor spheroids which coincided with an increase in P-gp expression as evaluated by semi-quantitative immunohistochemistry (Fig. 5A,B; n = 3).

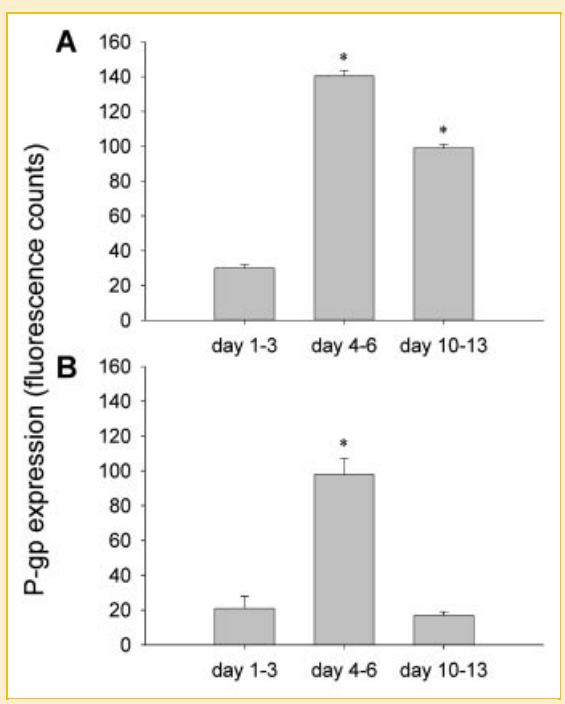


Fig. 4. Expression of P-gp in DU-145 (A) and Gli36 (B) multicellular tumor spheroids. The expression of P-gp is transient and occurs with the development of quiescent cell layers in the depth of the tissue. *$P < 0.05$, statistically different as compared to days 1–3 of cell culture (one-way ANOVA).

## CORRELATION OF GLYCOLYSIS AND THE INTRACELLULAR REDOX STATE OF TUMOR SPHEROIDS

Former studies of our group demonstrated that the intracellular redox state within tumor spheroids is closely related to P-gp expression [Wartenberg et al., 2001b]. Since the working hypothesis of the present study suggested that P-gp expression and the intracellular redox state may be correlated to glycolytic metabolism we investigated whether either exogenous addition of the glycolysis product pyruvate to the cell culture medium (Fig. 6; n = 3) or inhibition of glycolysis (Fig. 7A,B; n = 3) would affect intracellular ROS levels in multicellular tumor spheroids. To assess whether 2-DDG and IA treatment would indeed inhibit glycolytic activity in tumor spheroids and whether this could be correlated with the intracellular redox state the pyruvate and lactate content of 14-day-old DU-145 (Fig. 8A,B, n = 3) and 5-day-old Gli36 tumor spheroids (Fig. 8C,D; n = 3) was determined. It was shown that indeed addition of 10 μM pyruvate to the cell culture medium of decreased endogenous ROS production in DU-145 tumor spheroids, thus suggesting that pyruvate may act as a free radical scavenger (see Fig. 6; n = 3). Furthermore, when glycolysis was inhibited by either the non-metabolizable glucose analog 2-DDG (5 μM) (Fig. 7A; n = 3) or IA (10 μM) (Fig. 7B; n = 3) which inhibits glyceraldehyde-3-phosphate dehydrogenase an increased ROS generation in DU-145 tumor spheroids was observed. This could be inhibited in the presence of the free radial scavenger ebselen (5 μM). The presence of ebselen under conditions of inhibition of glycolysis did not affect lactate and pyruvate content of tumor spheroids (see Fig. 8A–D), indicating that glycolysis products are regulating the intracellular redox state of tumors, whereas glycolysis per se is not affected by ROS. Taken together these data clearly demonstrated that glycolysis is regulating the intracellular redox state of tumor spheroids, presumably by the generation of pyruvate which is well known to exert anti-oxidative properties [Brand and Hermfisse, 1997; Dobsak et al., 1999]. During the 24 h incubation period with glycolysis inhibitors no cytotoxic effects of the compounds were observed (data not shown).

## UPREGULATION OF P-gp EXPRESSION AND INCREASE OF DOXORUBICIN EFFLUX UPON TREATMENT OF TUMOR SPHEROIDS WITH PYRUVATE

The data of the present study demonstrated that pyruvate decreased intracellular ROS levels which should result in upregulation of P-gp. To assess this assumption tumor spheroids of the KB-3-1 cell line were treated from day 2 to day 10 of cell culture with either 10 μM or 1 mM pyruvate and P-gp–EGFP fluorescence, P-gp immunofluorescence and doxorubicin retention was monitored (Fig. 9A,B). It was evident that pyruvate treatment dose-dependent increased P-gp–EGFP fluorescence (evaluated at day 10 of cell culture), indicating enhanced P-gp expression (see Fig. 9A, n = 50 tumor spheroids). This was confirmed by semi-quantitative immunohistochemistry of P-gp (data not shown). Consequently in tumor spheroids treated for 8 days with either 10 μM or 1 mM pyruvate and subsequently with 5 μM doxorubicin for 3 h a decreased accumulation of the dye as well as doxorubicin retention 30 min after washout was observed

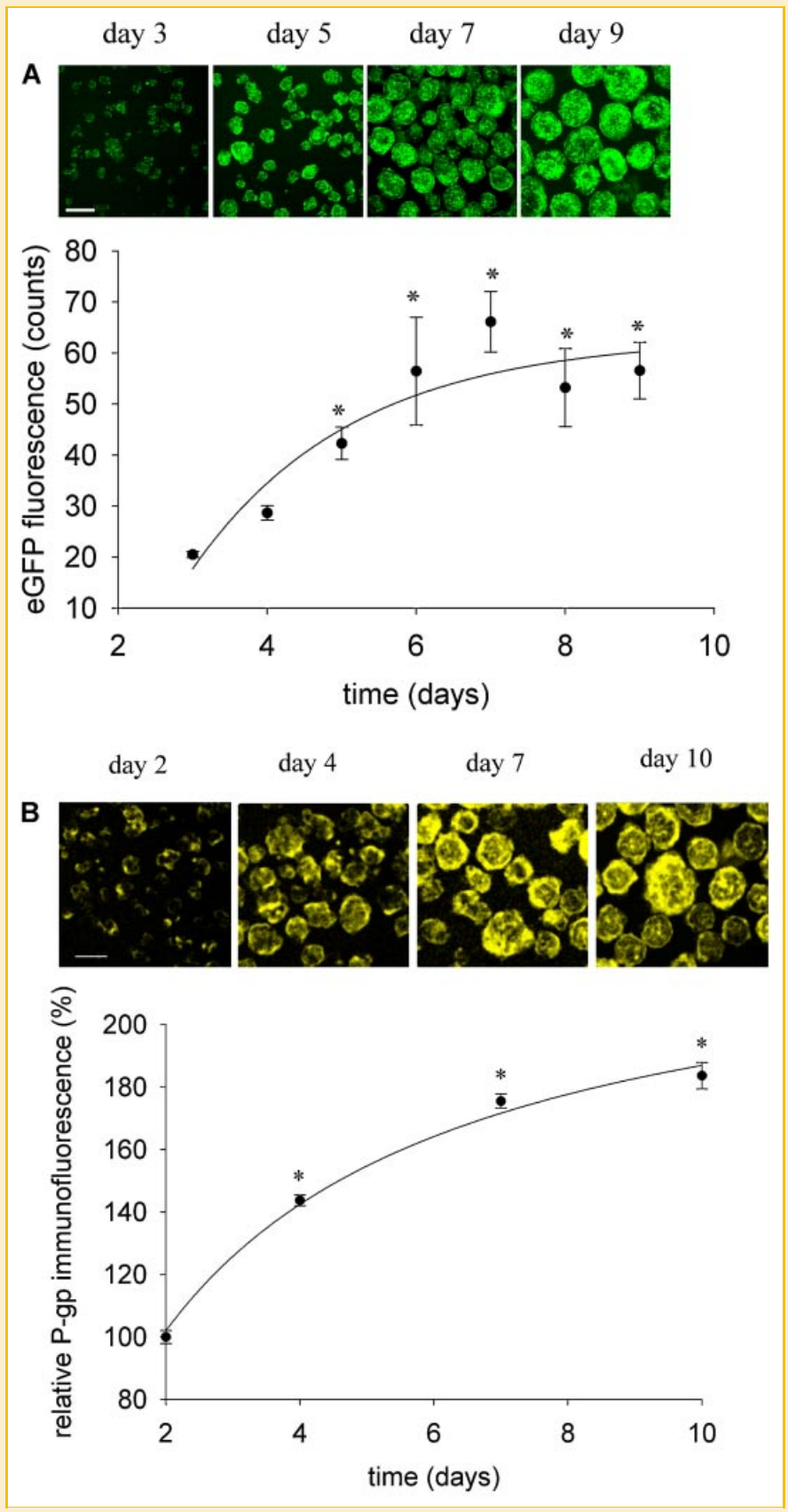


Fig. 5. P-gp–EGFP fluorescence (A) and semi-quantitative immunofluorescence of P-gp expression (B) in growing KB-3-1 multicellular tumor spheroids. Note, that P-gp–EGFP fluorescence increases with the size of tumor spheroids and well correlates to the data achieved with semi-quantitative immunohistochemistry. The bar represents 200 μM. $^{*}P < 0.05$, statistically different as compared to the first point in the curve (one-way ANOVA). [Color figure can be viewed in the online issue, which is available at www.interscience.wiley.com.]

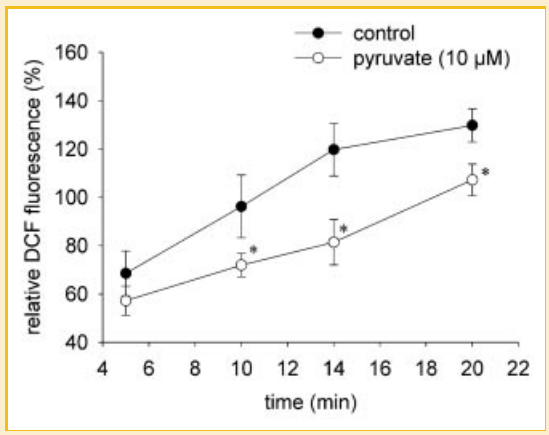


Fig. 6. Decrease in ROS generation following incubation of DU-145 multicellular tumor spheroid with 10 μM pyruvate. Pyruvate decreases intracellular ROS levels, suggesting that this glycolysis product acts as a free radical scavenger in multicellular tumor spheroids. $^{*}P < 0.05$, statistically different as compared to the untreated control (one-way ANOVA).

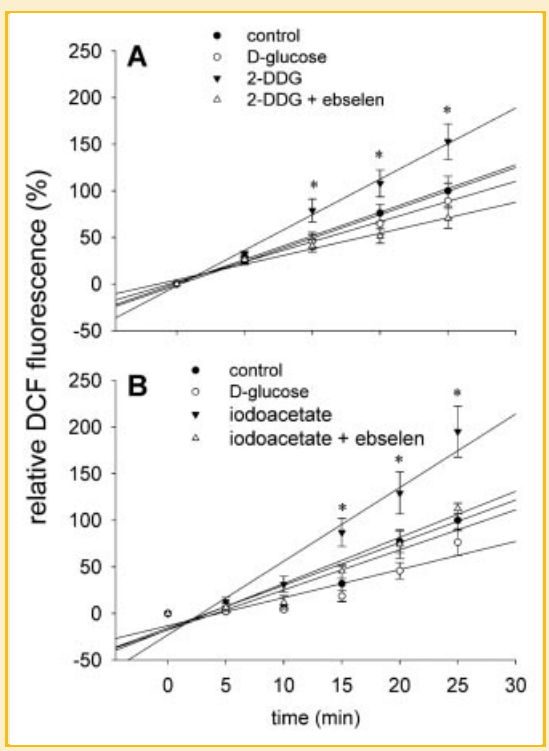


Fig. 7. Increase in the kinetics of ROS generation in multicellular DU-145 tumor spheroids upon inhibition of glycolysis with either 2-DDG (A) or iodoacetate (IA) (B). It is apparent that inhibition of glycolysis increases ROS generation, suggesting that glycolysis intermediates, presumably pyruvate are acting as free radical scavengers. The effect of glycolysis inhibition on ROS generation can be reversed upon incubation with the free radical scavenger ebselen. Addition of glucose (5 μM) is without effects on ROS generation. $^{*}P < 0.05$, statistically different as compared to untreated control (one-way ANOVA).

(see Fig. 9B, n = 50 tumor spheroids). This indicated that the increased P-gp expression correlated with function of the MDR transporter.

## EFFECTS OF GLYCOLYSIS INHIBITION ON THE EXPRESSION OF P-gp IN TUMOR SPHEROIDS

According to our working hypothesis pyruvate generated during glycolysis in multicellular tumor spheroids is upregulating P-gp expression through its anti-oxidative effects. Therefore it should be assumed that upon inhibition of glycolysis, that is, under conditions of increased intracellular ROS levels a decrease of P-gp expression occurs, which—if associated to a change in the intracellular redox state—should be reversible in the presence of ebselen. To validate this assumption 14-day-old DU-145 as well as 5-day-old Gli36 tumor spheroids were treated for 24 h with either 2-DDG (5 μM) or IA (10 μM) either in the presence or absence of ebselen, and P-gp expression was analyzed by semi-quantitative immunohistochemistry. Furthermore, EGFP fluorescence was determined in living 10-day-old KB-3-1 tumor spheroids under the same conditions by using the optical probe technique, which was previously established by us to assess drug resistance profiles in thick specimen [Wartenberg et al., 1998b]. As shown in Figure 10A,B expression of P-gp was significantly decreased upon incubation with 2-DDG and IA in DU-145 (see Fig. 10A, n = 3) and Gli36 (see Fig. 10B, n = 3) multicellular tumor spheroids. Co-incubation with the radical scavenger ebselen significantly reversed P-gp downregulation. To further validate our hypothesis that metabolic pathways determine P-gp expression via ROS we measured EGFP fluorescence in transfected KB-3-1 tumor spheroids following incubation with 2-DDG and IA. This was achieved by optical probe measurements using confocal laser scanning microscopy which allows the determination of GFP fluorescence in the depth of thick specimen after correction for light absorption with increasing penetration depth of the laser beam within the tissue (Fig. 11A–D; n = 3) [Wartenberg et al., 2001b]. It was apparent that KB-3-1 tumor spheroids displayed increased P-gp expression in the depth of the tissue which reached maximum values at a depth of 70–90 μm. Incubation with either 2-DDG or IA significantly decreased P-gp expression thus corroborating the immunohistochemical data obtained with DU-145 and Gli36 tumor spheroids.

## EFFECTS OF GLYCOLYSIS INHIBITION ON DOXORUBICIN RETENTION IN DU-145 TUMOR SPHEROIDS

Inhibition of glycolysis should impair P-gp function, since ATP generated through glycolysis is necessary for P-gp-ATPase activity. To validate this assumption 10-day-old DU-145 tumor spheroids were loaded for 90 min with 5 μM doxorubicin either in the presence or absence of 2-DDG or IA and ebselen, and doxorubicin fluorescence was determined 30 min after washout of the compound from the incubation medium (Fig. 12, n = 3). It was apparent that in the control samples doxorubicin was readily extruded from the tumor tissue due to the activity of P-gp which utilizes doxorubicin as a substrate. In contrast incubation of tumor spheroids with either 2-DDG or IA significantly increased doxorubicin retention which should result in increased cytotoxicity.

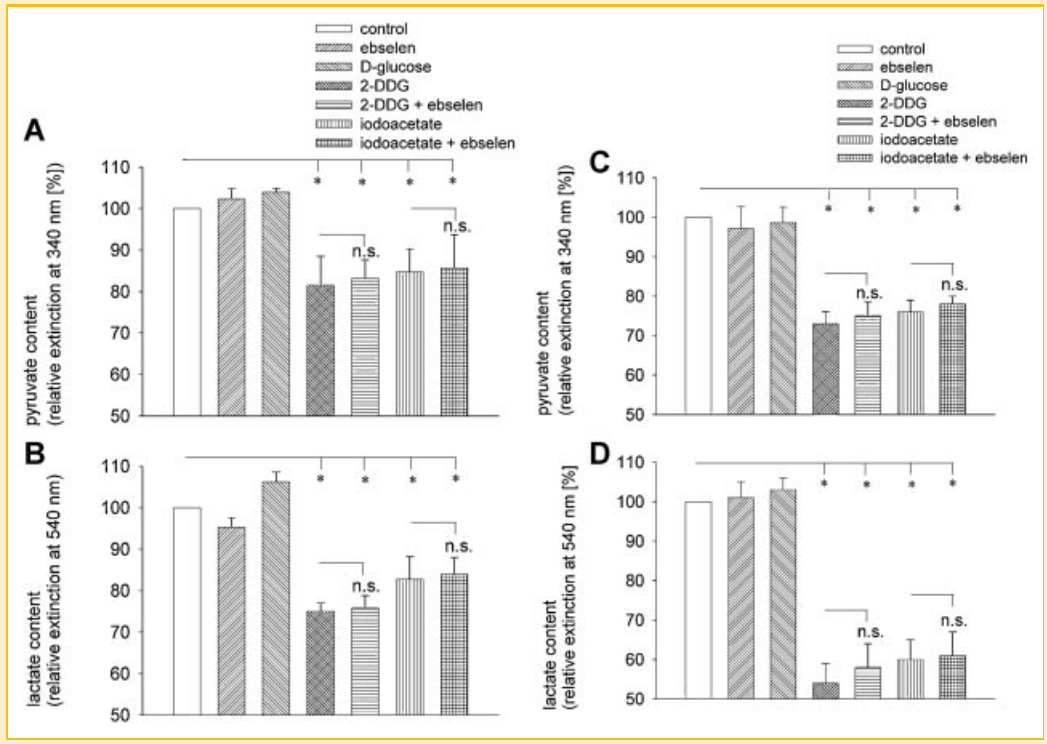


Fig. 8. Inhibition of pyruvate (A,C) and lactate (B,D) generation in 14-day-old DU-145 (A,B) and 5-day-old Gli36 (C,D) multicellular tumor spheroids upon inhibition of glycolysis with 2-DDG and iodoacetate (IA). Both compounds significantly inhibited pyruvate and lactate content. This inhibition was not impaired in the presence of the free radical scavenger ebselen and upon addition of exogenous glucose to the system. $^{*}P < 0.05$, statistically different as compared to untreated control (Student's *t*-test; n.s., not significant).

Ebselen did not impair doxorubicin retention, indicating that in contrast to P-gp expression P-gp function is not regulated by the intracellular redox state.

## DISCUSSION

Cancer cells exhibit an altered metabolism that is characterized by elevated uptake of glucose and increased glycolytic rates. This so called Warburg effect named after Otto Warburg who first reported on this phenomenon [Warburg, 1925] results in an increase in the production of pyruvate and/or lactate. Recent clinical evidence has pointed out that primary tumors, such as cervix carcinomas, head and neck squamous cell carcinomas or rectum adenocarcinomas, exhibit elevated lactate levels as a mirror of a high glycolytic activity, and are correlated even at the initial diagnosis with a high level of malignancy as indicated by increased formation of metastases or an elevated radiotherapy resistance [Sattler et al., 2007]. The metabolic shift towards glycolysis is at least partially mediated by tumor hypoxia and activation of HIF-1, a transcription factor that has been attributed prominent roles in tumorigenesis, angiogenesis, expression of glycolytic genes, and tumor survival [Young and Anderson, 2008]. HIF-1 is closely related to the expression of MDR genes that allow the effective extrusion of catabolic waste products from the hypoxic tumor tissue and to defend the cells against pro-apoptotic stimuli. Recently it has been hypothesized that the relationship between therapeutic resistance and glycolysis may at least partially be due to the radical scavenging potential of glycolytic intermediates, mainly pyruvate and to the link between these metabolites and the cellular redox status [Sattler et al., 2007].

In the present study we investigated the relation between glycolytic activity, generation of ROS and expression of P-gp. In previous studies we and others have demonstrated that P-gp expression is closely related to HIF-1α expression [Comerford et al., 2002] and the intracellular redox state [Wartenberg et al., 2003]. It was evidenced that upon exogenous addition of low levels of ROS P-gp was efficiently downregulated and the MDR phenotype reversed. From these data it was hypothesized that the decrease in endogenous ROS generation occurring with increased size of spheroids and development of P-gp expressing quiescent cell layers may be due to downregulation of the free radical scavenger pyruvate which is converted to lactate under hypoxic conditions. The data of the current study show that during the growth of multicellular tumor spheroids pyruvate generation was in deed downregulated, paralleled by increased lactate production. This scheme mirrors the development of hypoxia with increasing tumor growth in this model system for avascular micrometastases [Wartenberg et al., 2001a]. Consequently, a transient upregulation of the glycolytic enzymes LDHA, PDHA1, and HK1 was observed in tumor spheroids, thus reflecting a distinct time window of increased glycolytic activity, presumably induced by hypoxia and HIF-1. HIF-1 is well

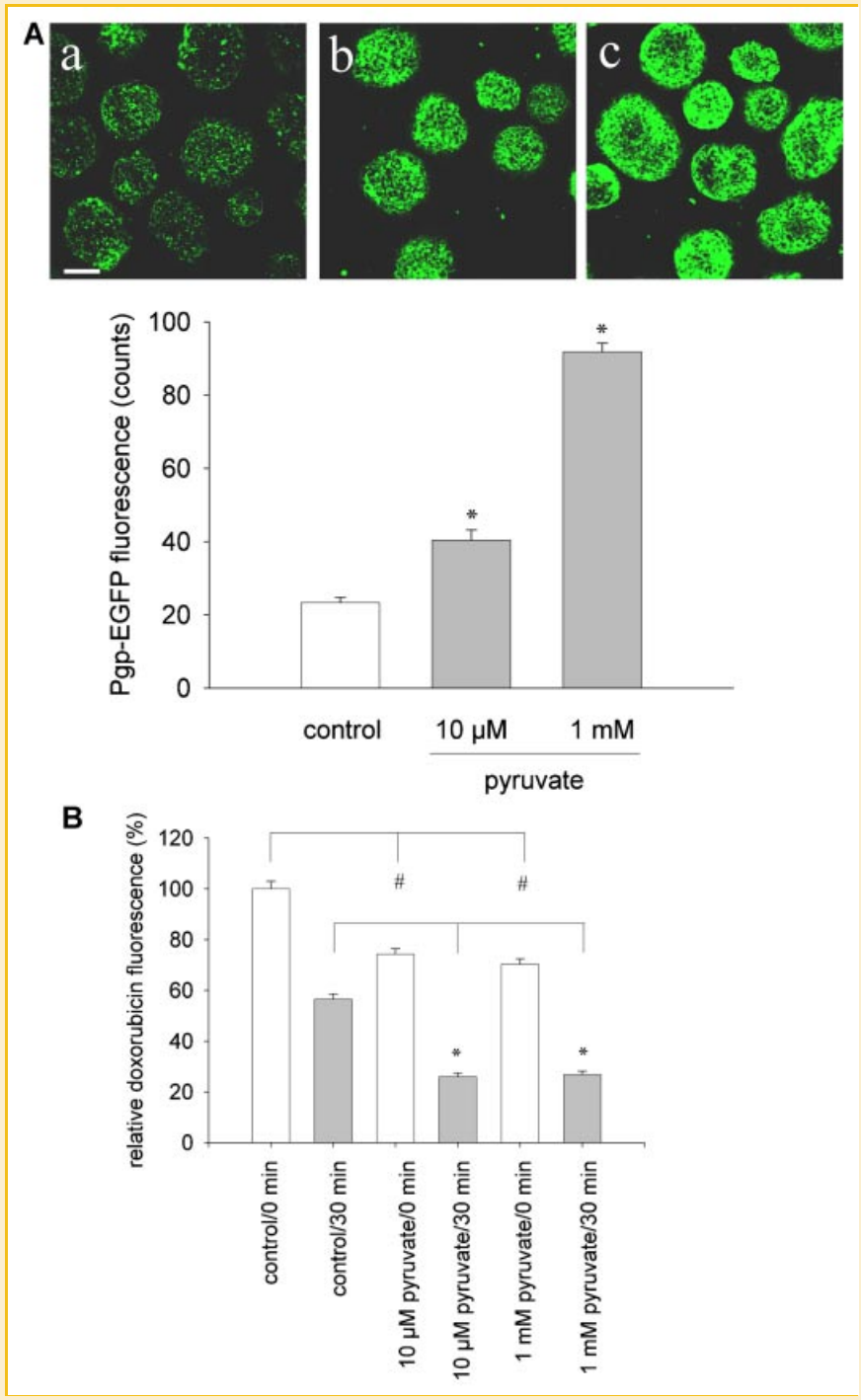


Fig. 9. Increase in P-gp–EGFP fluorescence (A) upon exogenous addition of either 10 μM or 1 mM pyruvate to the cell culture medium of KB-3-1 multicellular tumor spheroids. Tumor spheroids were treated from day 2 to day 10 of cell culture with pyruvate (10 μM, 1 mM) and EGFP fluorescence was evaluated on day 10. B: Doxorubicin (5 μM) uptake and retention in 10-day-old KB-3-1 tumor spheroids which remained either untreated (control) or were treated with 10 μM or 1 mM pyruvate. Tumor spheroids were loaded for 3 h with doxorubicin and fluorescence was evaluated (0 min). Subsequently doxorubicin was removed and fluorescence was monitored after 30 min. Note, that pyruvate treatment decreased doxorubicin uptake at 0 min and retention at 30 min, thus indicating increased doxorubicin export by P-gp. $^{*,\#}P < 0.05$, statistically different as indicated (one-way ANOVA). [Color figure can be viewed in the online issue, which is available at www.interscience.wiley.com.]

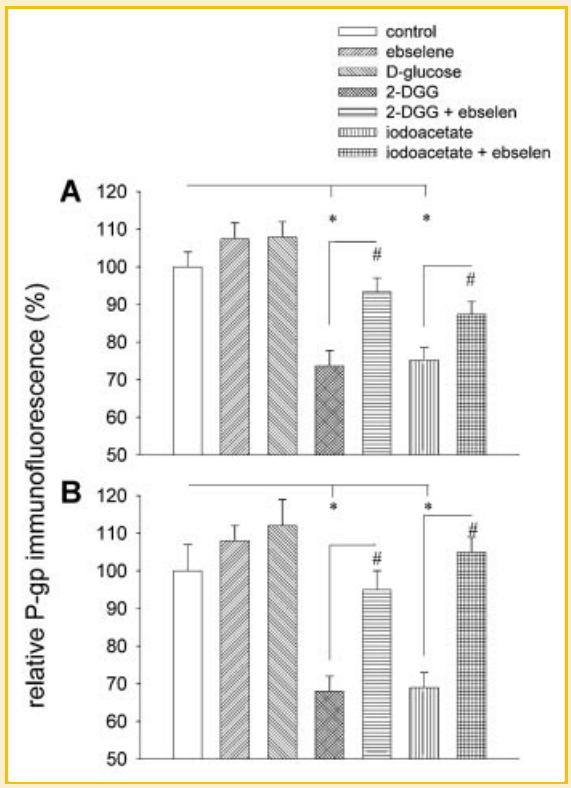


Fig. 10. Downregulation of P-gp expression in (A) 14-day-old DU-145 tumor spheroids and (B) 5-day-old Gli36 tumor spheroids upon inhibition of glycolysis by 2-DDG and iodoacetate. P-gp expression was analyzed by semi-quantitative immunohistochemistry. Note, that 2-DDG as well as iodoacetate significantly downregulated P-gp expression which was reversed upon co-incubation with the free radical scavenger ebselen, which indicates that P-gp expression is regulated by the intracellular redox state. $^{*,\#}P < 0.05$, statistically different as indicated (Student's *t*-test).

known to regulate the expression of several glycolytic genes [Bartrons and Caro, 2007]. Our data furthermore show that during growth of tumor spheroids P-gp is transiently upregulated in DU-145 and Gli36 and remained at an elevated level in KB-3-1 tumor spheroids which may be related to the fact that KB-3-1 only grow to sizes of approximately 300 μm, where central necrosis is not yet prevalent. In contrast Gli36 and DU-145 tumor spheroids grow to sizes of approximately 500 μm where central necrosis is prominent and increased generation of ROS occurs. This endogenous ROS generation in tumor spheroids with central necrosis may contribute to the downregulation of P-gp observed above all in 10- to 13-day-old Gli36 tumor spheroids which display an increased growth kinetics as compared to the DU-145 and KB-3-1 tumor spheroids investigated in the present study [Wartenberg et al., 2001b].

The transient expression of P-gp in multicellular tumor spheroids may be due to the anti-oxidant properties of pyruvate which was elevated in small tumor spheroids and exchanged against lactate with increasing size of spheroids and time of cell culture. The anti-oxidant properties of pyruvate have been recently demonstrated to protect human neuroblastoma cells against hydrogen peroxide-mediated apoptosis [Jagtap et al., 2003] and to protect mitochondria from oxidative stress [Wang et al., 2007]. Via its anti-oxidative properties pyruvate may enable the tumor cells to survive in a pro-apoptotic, hypoxic microenvironment. In the present study indeed exogenous pyruvate addition to the cell culture medium decreased endogenous ROS generation in DU-145 tumor spheroids, thus supporting our hypothesis that P-gp expression may be correlated to intracellular pyruvate levels and its anti-oxidative capacity. In a next step it was investigated whether pyruvate is involved in the expression of P-gp during the growth of tumor spheroids and whether inhibition of pyruvate generation would consequently downregulate P-gp. This was achieved by growing DU-145 and Gli36 tumor spheroids in the presence of the glycolysis inhibitors 2-DDG and IA. In fact these experimental conditions resulted in decreased pyruvate as well as lactate levels, suggesting effective inhibition of glycolytic activity. When ROS generation in the presence of glycolysis inhibition was assessed, it was apparent that 2-DDG as well as IA significantly increased ROS generation, thus supporting the notion that glycolysis metabolites are effectively scavenging intracellular ROS in tumor spheroids which is reversed in the presence of glycolysis inhibitors. Finally, when P-gp expression was investigated following culture of tumor spheroids under conditions of glycolysis inhibition (i.e., in the presence of either 2-DDG or IA) a significant downregulation of P-gp expression was observed. In corroboration of our assumption of a redox-control of P-gp regulation the free radical scavenger ebselen reversed the downregulation of P-gp expression observed with 2-DDG and IA. Furthermore exogenous addition of pyruvate to the cell culture medium increased P-gp expression and decreased doxorubicin retention. These findings clearly demonstrate that the down-regulation of P-gp expression upon glycolysis inhibition represents not a direct effect of this metabolic pathway but an indirect effect arising from an increase of ROS generation, presumably due to the downregulation of the free radical scavenger pyruvate. The data achieved by quantitative immunohistochemistry were confirmed by analysis of P-gp–EGFP expression in KB-3-1 cells and the optical probe technique which allows quantification of fluorescence labeled proteins in thick living specimen [Wartenberg et al., 1998b]. The P-pg-EGFP tumor spheroid model supplemented and broadened the evidence of the present study on P-gp expression in DU-145 and Gli36 tumor tissues under conditions of glycolysis inhibition obtained with conventional immunological techniques, since it allows quantification of P-gp expression and its regulation in different depth of a tumor tissue. The data on P-gp–EGFP expression in KB-3-1 tumor spheroids furthermore corroborated previous data of us suggesting that ROS are regulating P-gp expression on the post-translational level (i.e., P-gp stability) [Wartenberg et al., 2005] since KB-3-1 cells have constitutive P-gp–EGFP expression from an integrated retroviral vector. The P-gp–EGFP tumor spheroid model facilitates routine screenings of P-gp reversing agents and permits the analysis of P-gp expression in living cells during treatment with directly cytotoxic anti-cancer agents or compounds targeting metabolic pathways.

Currently anti-cancer strategies are developed which exploit the increased glycolytic activity of the tumor and intend to use glycolytic inhibitors in combinations with inhibitors directed against other metabolic processes [Denko, 2008]. Furthermore, recent studies demonstrated that glycolytic inhibitors at sublethal

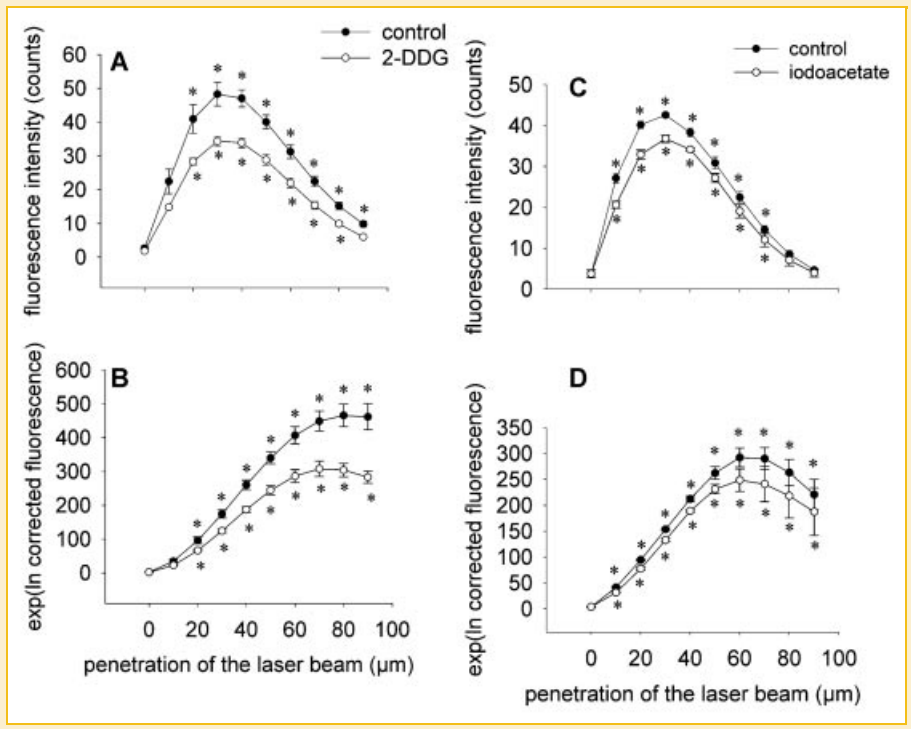


Fig. 11. Analysis of P-gp–EGFP fluorescence in the different depths of living KB-3-1 multicellular tumor spheroids upon inhibition of glycolysis by either 2-DDG (A,B) or iodoacetate (C,D) by using the optical probe technique. A,C: Original data which have to be corrected for light attenuation and scattering in the depth of the tissue as described in the Materials and Methods Section. B,D: Corrected data, which demonstrate that upon inhibition of glycolysis P-gp–EGFP is downregulated within the depth of the tumor tissue. $^{*}P < 0.05$, statistically different as compared to the first point in the respective curve (periphery of the tumor spheroid) (one-way ANOVA).

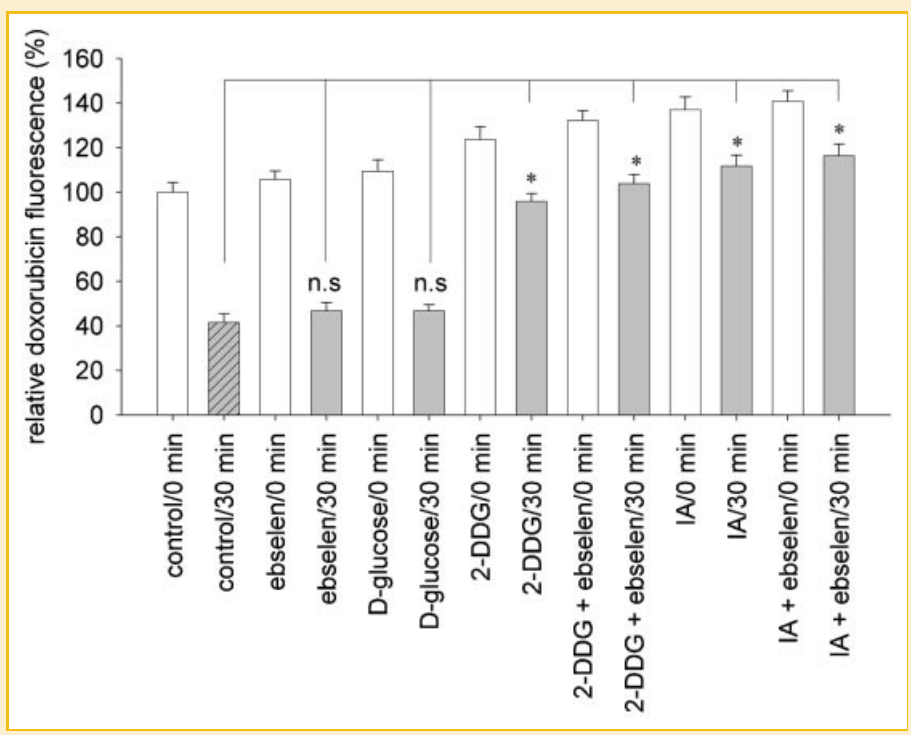


Fig. 12. Doxorubicin retention upon incubation of DU-145 multicellular tumor spheroids with the glycolysis inhibitors 2-DDG and iodoacetate (IA) either in the absence or presence of the free radical scavenger ebselen. Note that doxorubicin retention was significantly increased upon inhibition of glycolysis. Under these conditions the support of P-gp with ATP from glycolysis is limited which affects P-gp function, thus resulting in increased P-gp retention. The free radical scavenger ebselen does not reverse the increased doxorubicin retention achieved upon glycolysis inhibition, suggesting that P-gp function in contrast to P-gp expression is not affected by the intracellular redox state. $^{*}P < 0.05$, statistically different as compared to untreated control at 30 min (striated gray bar) (n.s., not significant) (one-way ANOVA).

doses sensitize tumor cells to conventional chemotherapy or radiotherapy [Maschek et al., 2004; Varshney et al., 2004]. These results have been explained with the notion that high rates of glycolysis are protecting against pro-apoptotic stimuli. Others have proposed that decreased mitochondrial function upon over-stimulation of glycolysis may alter apoptotic signaling through the mitochondria [Denko, 2008]. The present study offers an alternative model that implicates that the glycolysis product pyruvate efficiently scavenges ROS generated through NADPH oxidases and the mitochondrial respiratory chain. In the absence of endogenous ROS generation P-gp is upregulated and confers resistance against apoptosis and chemotherapeutic treatment regimen. In this model inhibition of glycolysis in tumors would not only kill tumor cells but would also chemosensitize the tumor. This would be achieved in parallel by downregulation of P-gp expression (through an increase in intracellular ROS) and by inhibition of P-gp function, which, as an ATPase, requires ATP generated by the glycolytic pathway. The parallel effect of glycolysis inhibitors on P-gp expression and function should render chemotherapy more efficient and avoid the reoccurrence of cancer subsequent to cancer treatment, which is mainly caused by the upregulation of MDR transporters.

## REFERENCES


Bartrons R, Caro J. 2007. Hypoxia, glucose metabolism and the Warburg's effect. J Bioenerg Biomembr 39:223–229.

Bentires-Alj M, Barbu V, Fillet M, Chariot A, Relic B, Jacobs N, Gielen J, Merville MP, Bours V. 2003. NF-kappaB transcription factor induces drug resistance through MDR1 expression in cancer cells. Oncogene 22:90–97.

Brand KA, Hermfisse U. 1997. Aerobic glycolysis by proliferating cells: A protective strategy against reactive oxygen species. FASEB J 11:388–395.

Chaiswing L, Zhong W, Cullen JJ, Oberley LW, Oberley TD. 2008. Extracellular redox state regulates features associated with prostate cancer cell invasion. Cancer Res 68:5820–5826.

Comerford KM, Wallace TJ, Karhausen J, Louis NA, Montalto MC, Colgan SP. 2002. Hypoxia-inducible factor-1-dependent regulation of the multidrug resistance (MDR1) gene. Cancer Res 62:3387–3394.

Dang CV. 2007. The interplay between MYC and HIF in the Warburg effect. Ernst Schering Found Symp Proc 4:35–53.

DeBerardinis RJ. 2008. Is cancer a disease of abnormal cellular metabolism? New angles on an old idea. Genet Med 10:767–777.

Denko NC. 2008. Hypoxia, HIF1 and glucose metabolism in the solid tumour. Nat Rev Cancer 8:705–713.

Dobsak P, Courderot-Masuyer C, Zeller M, Vergely C, Laubriet A, Assem M, Eicher JC, Teyssier JR, Wolf JE, Rochette L. 1999. Antioxidative properties of pyruvate and protection of the ischemic rat heart during cardioplegia. J Cardiovasc Pharmacol 34:651–659.

Jagtap JC, Chandele A, Chopde BA, Shastry P. 2003. Sodium pyruvate protects against H(2)O(2) mediated apoptosis in human neuroblastoma cell line-SK-N-MC. J Chem Neuroanat 26:109–118.

Maschek G, Savaraj N, Priebe W, Braunschweiger P, Hamilton K, Tidmarsh GF, De Young LR, Lampidis TJ. 2004. 2-deoxy-D-glucose increases the efficacy of adriamycin and paclitaxel in human osteosarcoma and non-small cell lung cancers in vivo. Cancer Res 64:31–34.

Mueller-Klieser W. 1997. Three-dimensional cell cultures: From molecular mechanisms to clinical applications. Am J Physiol 273:C1109–C1123.

Petriz J, Gottesman MM, Aran JM. 2004. An MDR-EGFP gene fusion allows for direct cellular localization, function and stability assessment of P-glycoprotein. Curr Drug Deliv 1:43–56.

Sattler UG, Walenta S, Mueller-Klieser W. 2007. Lactate and redox status in malignant tumours. Anaesthesist 56:466–469.

Sauer H, Wartenberg M, Hescheler J. 2001. Reactive oxygen species as intracellular messengers during cell growth and differentiation. Cell Physiol Biochem 11:173–186.

Scatena R, Bottoni P, Pontoglio A, Mastrototaro L, Giardina B. 2008. Glycolytic enzyme inhibitors in cancer treatment. Expert Opin Invest Drugs 17:1533–1545.

Sharom FJ. 2008. ABC multidrug transporters: Structure, function and role in chemoresistance. Pharmacogenomics 9:105–127.

Thevenod F, Friedmann JM, Katsen AD, Hauser IA. 2000. Up-regulation of multidrug resistance P-glycoprotein via nuclear factor-kappaB activation protects kidney proximal tubule cells from cadmium- and reactive oxygen species-induced apoptosis. J Biol Chem 275:1887–1896.

Varshney R, Gupta S, Dwarakanath BS. 2004. Radiosensitization of murine Ehrlich ascites tumour by a combination of 2-deoxy-D-glucose and 6-aminonicotinamide. Technol Cancer Res Treat 3:659–663.

Wang X, Perez E, Liu R, Yan LJ, Mallet RT, Yang SH. 2007. Pyruvate protects mitochondria from oxidative stress in human neuroblastoma SK-N-SH cells. Brain Res 1132:1–9.

Warburg O. 1925. Uber den Stoffwechsel der Carcinomzelle. Klin Wochenschr 4:534–536.

Wartenberg M, Frey C, Diedershagen H, Ritgen J, Hescheler J, Sauer H. 1998a. Development of an intrinsic P-glycoprotein-mediated doxorubicin resistance in quiescent cell layers of large, multicellular prostate tumour spheroids. Int J Cancer 75:855–863.

Wartenberg M, Hescheler J, Acker H, Diedershagen H, Sauer H. 1998b. Doxorubicin distribution in multicellular prostate cancer spheroids evaluated by confocal laser scanning microscopy and the ''optical probe technique''. Cytometry 31:137–145.

Wartenberg M, Fischer K, Hescheler J, Sauer H. 2000. Redox regulation of P-glycoprotein-mediated multidrug resistance in multicellular prostate tumour spheroids. Int J Cancer 85:267–274.

Wartenberg M, Donmez F, Ling FC, Acker H, Hescheler J, Sauer H. 2001a. Tumour-induced angiogenesis studied in confrontation cultures of multicellular tumour spheroids and embryoid bodies grown from pluripotent embryonic stem cells. FASEB J 15:995–1005.

Wartenberg M, Ling FC, Schallenberg M, Baumer AT, Petrat K, Hescheler J, Sauer H. 2001b. Down-regulation of intrinsic P-glycoprotein expression in multicellular prostate tumour spheroids by reactive oxygen species. J Biol Chem 276:17420–17428.

Wartenberg M, Ling FC, Muschen M, Klein F, Acker H, Gassmann M, Petrat K, Putz V, Hescheler J, Sauer H. 2003. Regulation of the multidrug resistance transporter P-glycoprotein in multicellular tumour spheroids by hypoxia-inducible factor (HIF-1) and reactive oxygen species. FASEB J 17:503–505.

Wartenberg M, Gronczynska S, Bekhite MM, Saric T, Niedermeier W, Hescheler J, Sauer H. 2005. Regulation of the multidrug resistance transporter P-glycoprotein in multicellular prostate tumour spheroids by hyperthermia and reactive oxygen species. Int J Cancer 113:229–240.

Wu WS. 2006. The signaling mechanism of ROS in tumour progression. Cancer Metastasis Rev 25:695–705.

Young CD, Anderson SM. 2008. Sugar and fat—that's where it's at: METABOLIC changes in tumours. Breast Cancer Res 10:202.